



# Reductions in nitrogen oxides over Europe driven by environmental policy and economic recession

Patricia Castellanos<sup>1</sup> & K. Folkert Boersma<sup>1,2</sup>

<sup>1</sup>Royal Netherlands Meteorological Institute, Climate Observations Department, De Bilt, The Netherlands, <sup>2</sup>Eindhoven University of Technology, Fluid Dynamics Lab, Eindhoven, The Netherlands.

Fuel combustion is a significant source of numerous air pollutants, which reduce local air quality, and affect global tropospheric chemistry. Satellite observations of nitrogen dioxide, emitted by combustion processes, allow for robust monitoring of atmospheric concentrations at high spatial resolution on continental scales. Here we evaluate changes in tropospheric NO<sub>2</sub> concentrations over Europe between 2004 and 2010. We isolate long-term (timescales greater than one year) variability in the daily NO<sub>2</sub> observations from the Ozone Monitoring Instrument (OMI) using a spectral analysis. In 2010, we find substantial reductions in NO<sub>2</sub> concentrations of at least 20% throughout Europe. These reductions are as much the result of temporary reductions prompted by the 2008–2009 global economic recession, as of European NO<sub>x</sub> emission controls. Our results demonstrate that realistic concentration pathways of NO<sub>2</sub> do not follow simple linear trends, but reflect a compilation of environmental policy and economic activity.

Nitrogen oxides (NO<sub>x</sub> = NO + NO<sub>2</sub>) play an important role in many atmospheric processes with strong implications for ecosystem stability, climate change, and public health. In polluted areas, NO<sub>x</sub> is produced in massive amounts by anthropogenic combustion primarily in the form of NO, which is rapidly transformed into NO<sub>2</sub> by reaction with ozone. During the daytime, photolysis of NO<sub>2</sub> leads to a steady state between NO and NO<sub>2</sub> such that under typical urban conditions, at midday, roughly half of NO<sub>x</sub> is in the form of NO<sub>2</sub>. In the lower atmosphere, NO<sub>x</sub> contributes to acid deposition as well as ozone and aerosol formation. Moreover, at high concentrations NO<sub>x</sub> is toxic.

Accurate knowledge of changes in NO<sub>x</sub> concentrations is essential in order to monitor the effectiveness of air pollution abatement strategies in the context of changes in economic activity. Conventional methods to measure NO<sub>x</sub> used in surface observation networks can produce poorly quantified high biases<sup>1–3</sup>. Surface sites are sparse, lack spatial representativity, and can be heavily influenced by nearby sources. Particularly over Europe, where NO<sub>x</sub> trends have been small over the last decade due to modest changes in emissions standards and economic growth compared to North America and east Asia<sup>4–6</sup>, trends inferred from these networks may not represent the true changes in NO<sub>x</sub> concentrations. Indeed, trends in European NO<sub>x</sub> emissions and surface monitored NO<sub>x</sub> have been inconsistent<sup>7–9</sup>.

Satellite observations of NO<sub>2</sub> tropospheric columns have become increasingly useful for observing trends in NO<sub>2</sub> concentrations<sup>4,10,11</sup> and inferring surface NO<sub>x</sub> emissions from particular sources<sup>12–16</sup> on regional and global scales<sup>17,18</sup>. Satellite observations cover a large area and provide an impartial, self-consistent time series of NO<sub>2</sub> concentrations. In the following we present trends in NO<sub>2</sub> concentrations over Europe measured with the Ozone Monitoring Instrument (OMI)<sup>19</sup> between October 2004 and December 2010 (see Methods). We use tropospheric NO<sub>2</sub> columns observed under ‘cloud free’ conditions (cloud fraction below 20%) at 13:40 hours local time (DOMINO v1.02, see Methods)<sup>20</sup>. The high spatial resolution and sampling frequency of OMI observations (down to 24 km × 13 km pixel size and daily global coverage) enable the detection of relatively small interannual variability within the NO<sub>2</sub> signal. Here we isolate the low frequency (having periodicity greater than 1.4 years) components in the 2004–2010 NO<sub>2</sub> time series by conducting a spectral analysis<sup>21</sup> on the daily observations as discussed in the Methods and illustrated (for the case of Madrid) in Figure 1, thus avoiding the need to make assumptions about the seasonal variability of NO<sub>2</sub> (e.g. Ref. 4 & 22), which could introduce errors in the estimate of the trend.

During the time period under consideration, the 2008–2009 global economic recession effectuated a distinct change in anthropogenic activity in Europe, indicated by sharp downturns in gross domestic product (GDP),

SUBJECT AREAS:  
ATMOSPHERIC SCIENCE  
ENVIRONMENTAL CHEMISTRY  
ENVIRONMENT  
EARTH SCIENCES

Received  
7 November 2011

Accepted  
25 January 2012

Published  
16 February 2012

Correspondence and  
requests for materials  
should be addressed to  
P.C. (castellanos.  
patricia@gmail.com)

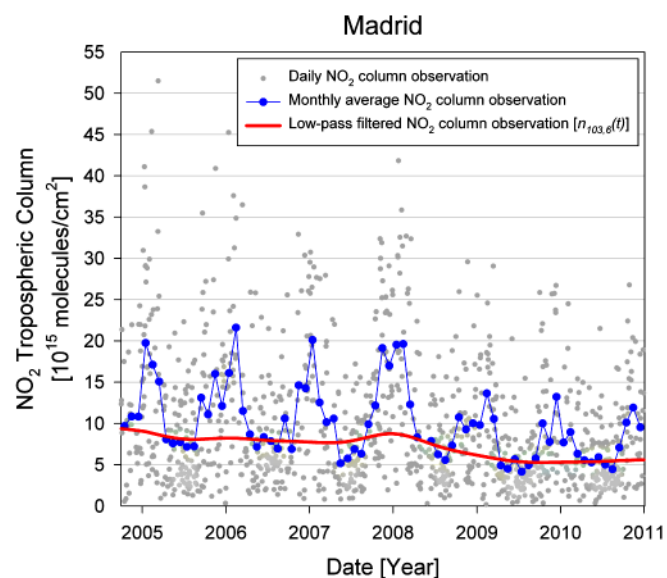


**Figure 1** | 2004–2010 timeseries of OMI tropospheric NO<sub>2</sub> column observations over the city of Madrid. Grey circles indicate daily observations and blue circles the monthly average for cloud-free conditions (cloud radiance fraction below 0.5). The red line shows the low-pass (KZ) filtered NO<sub>2</sub> column signal as a result of 6 iterations of a 103-day moving average filter ( $n_{103,6}(t)$ ) (see Methods).

industrial production, and construction<sup>23</sup>. Presumably this lead to an analogous decrease in NO<sub>x</sub> emissions associated with these activities in addition to continuing NO<sub>x</sub> emissions reductions related to the implementation of new technology as determined by local and European wide emissions control strategies<sup>24</sup>. We apply here a simple regression model to the multi-year changes in NO<sub>2</sub> concentration in order to distinguish between the impact of environmental policy and the economic recession on air quality over Europe.

## Results

**Multi-year changes in tropospheric NO<sub>2</sub> columns.** Figure 2 shows August average low-pass filtered OMI tropospheric NO<sub>2</sub> columns over Europe. NO<sub>2</sub> concentrations in 2005 are particularly high in densely populated and industrial areas. The observations indicate that NO<sub>2</sub> concentrations declined by up to 20% between 2005 and 2008 in many polluted regions (e.g. Germany, the Netherlands, Belgium, Italy, Spain), but increased by up to 15% over the North Sea and eastern Europe. In the year 2009, NO<sub>2</sub> concentrations are at least 10% lower than 2005 values everywhere, but 20–40% lower than 2005 values in industrialized regions of Germany, the Po Valley, northwestern Spain, and large cities. This across the board reduction in NO<sub>2</sub> coincides with the change in anthropogenic activity associated with the global economic recession. By the end of 2010, economic indicators for many European countries began to return to pre-recession levels. Reductions in NO<sub>2</sub> concentrations generally slowed down in 2010, possibly indicating the beginning of economic recovery. Overall, NO<sub>2</sub> concentrations at the end of 2010 are 20–30% lower than in 2005; with few exceptions, air quality over Europe has improved.

**Environmental policy vs economic recession: regression modeling.** Over Europe we expect that changes in NO<sub>2</sub> columns respond proportionally to changes in NO<sub>x</sub> emissions<sup>5,25</sup>. Although gradual reductions in NO<sub>x</sub> emissions over 2004–2009 have been reported to the European Environment Agency (EEA)<sup>26</sup>, suggesting a linear trend in NO<sub>x</sub> emissions and NO<sub>2</sub> concentrations, the clear nonlinearity in the 2008–2009 changes in NO<sub>2</sub> concentration intimates that some of the air quality improvements by the end of 2010 are independent of

European environmental policy and may be associated with economic recession. Thus we attempt to separate the observed NO<sub>2</sub> multi-year changes into recession and ‘business-as-usual’ components.

We fit the first derivative of low-pass filtered observed NO<sub>2</sub> columns ( $\frac{dn_{103,6}}{dt}$ ) to Eqn. 1 (see Supplementary Information: ‘Regression Modeling’). We assume NO<sub>2</sub> concentrations are changing at a constant rate ( $c_{continuous}$ ) throughout 2004–2010 as a result of the competition between stable economic growth and continuing vehicle turnover and installation of control technology at point sources. For the period of economic recession, we implement an additional reduction ( $c_{recession}$ ), which we assume lasts for one year and is centered on the minimum observed NO<sub>2</sub> first derivative occurring after 2008 in each grid cell.

$$\frac{dn_{103,6}}{dt} = \begin{cases} c_{continuous} & t \notin recession \\ c_{continuous} + c_{recession} & t \in recession \end{cases} \quad (1)$$

The timing of the recession term is allowed to vary between grid cells in order to account for variability in local economies. We assume the rate of NO<sub>2</sub> changes return to pre-2008 levels after the recession.

**Comparison of policy and recession driven NO<sub>2</sub> changes.** Figure 3 shows the fitted and observed low-pass filtered NO<sub>2</sub> concentrations averaged over the UK, Netherlands, Belgium, and northern France, the region of highest NO<sub>2</sub> concentrations in Europe (area delineated by white box in Figure 2(top left)). During the estimated local recession time period (starting between June 2007 and October 2008 for that region), it is apparent that observed NO<sub>2</sub> reductions are accelerating. By fitting the NO<sub>2</sub> first derivative to Eqn. 1 we are able to reproduce the observed variability (Figure 3). If the small pre-recession trends in this region, as calculated from the regression fit, had continued through 2010, the reduction in NO<sub>2</sub> concentrations would have been only 2–4% as opposed to the observed ~15%. Thus a large fraction of the improvements in air quality over northwestern Europe by 2010 are likely a result of NO<sub>x</sub> emissions reductions driven by episodic economic downturns.

Fluctuations in the low-pass filtered NO<sub>2</sub> concentration suggest that meteorological variability may have influenced apparent changes in tropospheric NO<sub>2</sub>. We find from regression modeling of the NO<sub>2</sub> first derivative with several meteorological parameters that while taking into account meteorological trends and/or variability resulted in a better fit to the data between 2004 and 2008, it had negligible influence on the calculated  $c_{continuous}$  and  $c_{recession}$  terms (to within their 95% confidence intervals) over most of Europe (see Supplementary Information).

The calculated total change in NO<sub>2</sub> associated with environmental policy ( $c_{continuous} \times 2283$  days - the length of the 2004–2010 OMI observation time series used here) is shown in Figure 4(left). Table S1 presents specific values for cities with populations greater than 500,000, labeled with black diamonds in Figure 4 as well as values for the locations of three power stations indicated with green boxes. In Germany, Spain, southern France, Italy, Austria, Hungary, and parts of western Poland we find 10–50% reductions in NO<sub>2</sub> concentration between 2004 and 2010. The strongest NO<sub>2</sub> reductions occur in industrial areas where large power plants are located, such as southwestern Germany, eastern Germany along the Polish border (where the largest German coal-fired power plant is located), northwestern Spain (~70% declines at the Compostilla II plant; green box in Figure 4), and the Po Valley, suggesting the installation of new NO<sub>x</sub> emissions controls and/or more efficient combustion technology. Figure 4(left) also indicates increased NO<sub>2</sub> (30–50%) around the largest cities in the UK, the English Channel, Ukraine, northeast Poland, and Turkey. Hot spots in Poland and Turkey correspond with construction of the Ostraleka Mill power station starting in 2008 and the upgrade of the Hamitabat power station, respectively (green boxes in Figure 4). Increased NO<sub>2</sub> concentrations in the areas surrounding London might be indicative of suburban development

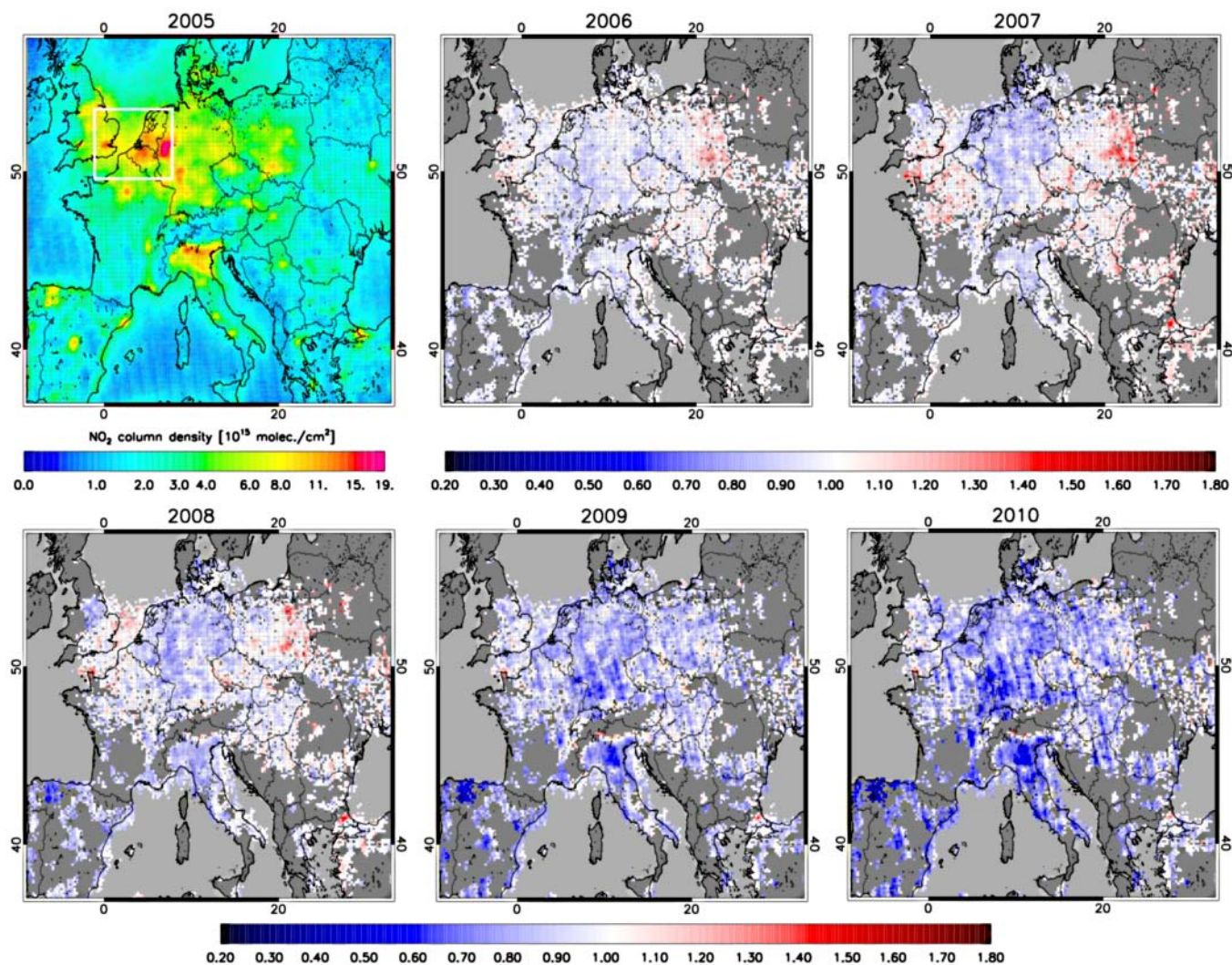


**Figure 2** | August 2005 average low-pass filtered OMI tropospheric  $\text{NO}_2$  columns ( $n_{103,6}$ ) (top left), and the 2006–2010 August average low-pass filtered  $\text{NO}_2$  columns normalized by August 2005 values. Grid cells are considered if less than 5% of the original data were invalidated and the resulting probability distribution does not differ significantly from the original data (Mann-Whitney U test,  $p = 0.05$  one-tailed) (See Supplementary Information).

(especially along the M11 highway corridor north of London), and increased motor vehicle traffic along the city's periphery in response to the 2007 congestion tax discouraging driving in the city center.

At the national scale, for most European countries we find the calculated business-as-usual  $\text{NO}_2$  changes are in line with trends in  $\text{NO}_x$  emissions reported to the EEA for 2004 to 2007 (Figure S5). However, positive  $\text{NO}_2$  trends over the UK are inconsistent with reported declining emissions, and the Netherlands, France, Czech Republic, and Belgium report stronger emissions reductions than suggested by the observed  $\text{NO}_2$  trend.

Figure 4(right) shows 10–30% one-year recession-driven  $\text{NO}_2$  reductions over most areas in Europe. The largest decreases in  $\text{NO}_2$  associated with the recession occur over the southern North Sea and English Channel (an area of intense ship traffic), as well as the UK, Poland, southern Germany, France, and Turkey. Figure 5 shows the European average time series of  $\text{NO}_2$  concentration with industrial production index (IPI) reported by the statistical office of the European Union (Eurostat). Industrial production index is an economic indicator for price-adjusted output of manufacturing, mining, and energy production.  $\text{NO}_2$  concentrations decline between 2004 and 2008 in spite of economic growth, clearly indicating the effectiveness of environmental policy. The recession period decline in IPI is correlated with and proportional to observed  $\text{NO}_2$

reductions at the national level, as illustrated by coincident 5–20% decreases in IPI and  $\text{NO}_2$  concentration for all European countries (lower left quadrant of Figure 5(left)), further indicating the role of economic downturn in improving air quality across Europe. Scatter in the ratios of recession period  $\text{NO}_2$  reduction to IPI in Figure 5 reflects country-to-country differences in (1) the ratio of  $\text{NO}_x$  emissions from industrial sources to transportation, (2) the dominant type of industry (differing ratios of activity to emissions), and (3) progress in implementation of  $\text{NO}_x$  emissions controls. Figures 3 and 5 show that as the European economy begins to recover, and industrial activity increases,  $\text{NO}_2$  reductions are likely to slow down.

In Figure 6 we compare total  $\text{NO}_2$  concentration changes before the recession to  $\text{NO}_2$  concentration changes during the recession (see Figure S6 for all cities). With the exception of London, Birmingham, Paris, Minsk, Helsinki, Hamburg, and Mykoliav, all of Europe's largest cities underwent net decreases in  $\text{NO}_2$  concentrations prior to the economic recession. Assuming that the ratio of a relative change in tropospheric  $\text{NO}_2$  to a relative change in  $\text{NO}_x$  emissions is approximately constant over 2004–2010 (Lamsal et al.<sup>25</sup> report that this ratio varies by less than 3%), the change in  $\text{NO}_2$  concentration during the recession divided by the business-as-usual change in  $\text{NO}_2$  leading up to the recession is comparable to the ratio of  $\text{NO}_x$  emissions changes during the two time periods. In general, reductions in

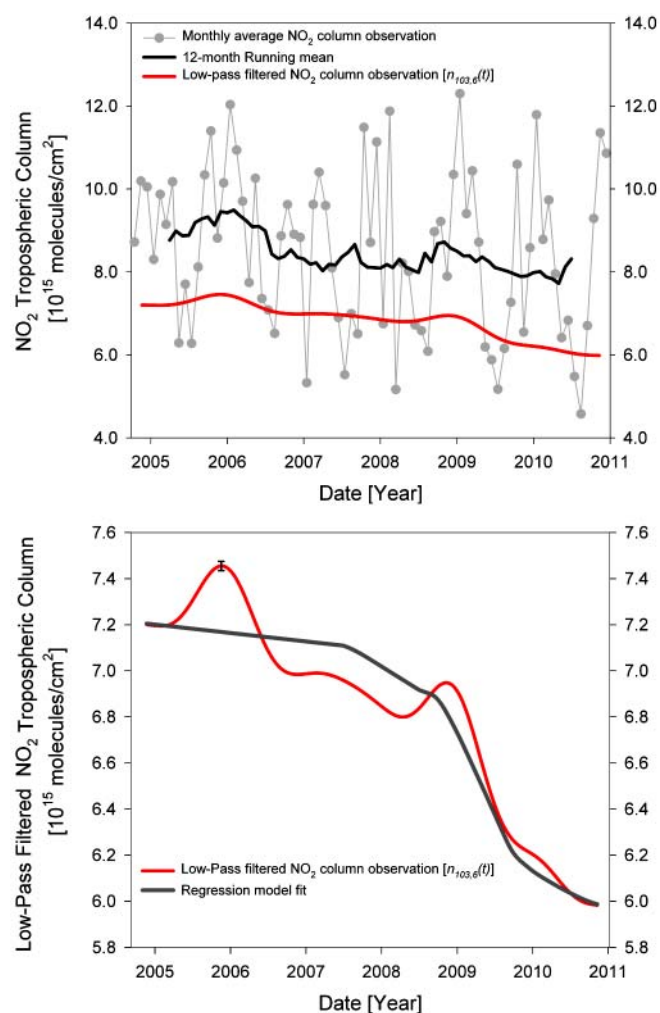


**Figure 3** | The top panel shows the observed monthly average  $\text{NO}_2$  column (grey circles) averaged over the eastern United Kingdom, Belgium, Luxembourg, and the Netherlands (area indicated by the white box in Figure 2(top left)) and their 12-month running mean (black line). The red line indicates the corresponding average low-pass filtered signal. The bottom panel shows again the Benelux-UK average low-pass filtered  $\text{NO}_2$  column (red line) with the fit of the regression model (Eqn. 1) to the data (grey). The uncertainty in the average observed  $\text{NO}_2$  column (black error bar) represents the precision of the spatial average over the Benelux-UK area. The measurement precision in each grid cell that is propagated when taking the average is derived by assuming  $\sigma=5\%$  as discussed in the Supplementary Information – “Regression Modeling”. The standard error in the average regression model fit is commensurate with the thickness of the line.

$\text{NO}_x$  emissions during the recession were equal to or greater than the total emissions reductions accumulated over the approximately four prior years. We find significant contributions to  $\text{NO}_2$  reductions from the economic recession occurring mostly in the first half of 2008 in southern Europe, and one year later in northern and eastern Europe, consistent with economic data (Figure 6 inset).

## Discussion

With daily tropospheric  $\text{NO}_2$  column observations from OMI, we are able to present spatially and temporally heterogeneous multi-year changes in  $\text{NO}_2$ . Overall, air quality over Europe has improved over the course of 2004–2010. Our regression modeling indicates that environmental policy measures drove 10–50% declines in  $\text{NO}_2$  over Europe between 2004 and 2010. That the

largest  $\text{NO}_2$  reductions occurred in industrialized areas (e.g.  $\sim 70\%$  declines at the Compostilla II power station in northwest Spain) confirms implementation of  $\text{NO}_x$  emissions controls obliged by policy measures. Areas where the calculated policy driven  $\text{NO}_2$  change is positive correspond to regions that have seen significant economic development and associated increases in fuel combustion; for example, the construction of the Ostraleka Mill power station in northwestern Poland, and the upgrade of the Hamitabat power station northwest of Istanbul have led to net increases in  $\text{NO}_2$  concentration ( $\sim 5\%$ ) despite the recession. Notably, the UK has reported decreasing  $\text{NO}_x$  emissions while  $\text{NO}_2$  concentrations have increased mostly surrounding London, suggesting increased pollution as a result of suburban development or motor vehicle congestion.

In 2009, the global recession accelerated  $\text{NO}_2$  reductions; European  $\text{NO}_2$  concentrations decreased by 15–30% relative to 2004 concentrations as a result of fast declines in  $\text{NO}_x$  emissions. Particularly, the shipping lane between the UK and continental Europe shows large decreases during the recession. The coastlines of the neighboring countries – Belgium, France, the Netherlands, and UK – follow the same trend. Modeling sensitivity studies focused on northern Europe show that emissions from ships may contribute about 10% to the surface  $\text{NO}_x$  concentration over land in the Netherlands, Belgium, northern France, and southern UK<sup>27</sup>. It is telling that these countries, whose emissions inventories are considered the most accurate in Europe, all show  $\text{NO}_2$  trends that are smaller than would be implied by their reported  $\text{NO}_x$  emissions reductions. While land based  $\text{NO}_x$  emissions from internal combustion engines have been subject to legislation for over 20 years, emissions from shipping have gone largely uncontrolled. Thus the lack of emissions controls on shipping emissions in the channel may be suppressing air quality improvements for Belgium, France, Netherlands, and UK.

In many large cities across Europe, the  $\text{NO}_x$  emissions reduction during roughly one year of economic downturn outweighed approximately 4 years of policy improvements. We found that rapid  $\text{NO}_2$  reductions generally correlate well with sharp reductions in industrial activity over Europe. These findings are of relevance to demonstrating that realistic  $\text{NO}_x$  emissions scenarios and  $\text{NO}_2$  concentration pathways do not follow simple linear trends, but instead reflect a compilation of environmental policy measures and economic activity, at least over Europe.

Because satellites offer global coverage, our method to analyze the observation time series can be applied to any region, city, or major point source worldwide. The independent and up-to-date monitoring of changes in  $\text{NO}_2$  concentrations that satellites provide will benefit from the continuation of ongoing observations and the improved spatial resolution from future (geostationary) satellite instruments.

## Methods

**Satellite Observations.** We use  $\text{NO}_2$  tropospheric vertical column densities from OMI<sup>19</sup> retrieved with the Dutch OMI  $\text{NO}_2$  algorithm (DOMINO) version 1.02 over Europe ( $37^\circ\text{N}$  to  $62^\circ\text{N}$  and  $-9^\circ\text{W}$  to  $33^\circ\text{E}$ ).  $\text{NO}_2$  tropospheric columns are derived with a three-step approach: (1)  $\text{NO}_2$  slant columns are retrieved with Differential Optical Absorption Spectroscopy in the 405–465 nm wavelength range (spectral resolution of 0.5 nm), (2) OMI  $\text{NO}_2$  slant columns are assimilated in the global chemistry transport model TM4<sup>28</sup>, which provides the stratospheric background and a priori  $\text{NO}_2$  profile shape needed to calculate the tropospheric air mass factor, which is used to (3) convert the tropospheric slant column into a vertical column<sup>20</sup>. The OMI pixel size varies from  $24\text{ km} \times 13\text{ km}$  at nadir to  $140\text{ km} \times 26\text{ km}$  at the edges of the swath. Individual pixels, weighted by the cosine of the viewing zenith angle, were re-gridded to  $0.125^\circ$  latitude by  $0.25^\circ$  longitude ( $\sim 14\text{ km} \times \sim 20\text{ km}$ ). Pixels affected by the row anomaly (tracks 27–44 and 53–54)<sup>29</sup> were excluded for the entire 2004–2010 time period.

**Isolating Multi-year Changes in  $\text{NO}_2$ : The KZ Filter.** To separate the  $\text{NO}_2$  time series into different frequency components, we use the Kolmogorov-Zurbenko (KZ) filter<sup>30</sup>. A KZ filter is simply  $k$  iterations of a successive moving average of window length ( $m$ ):

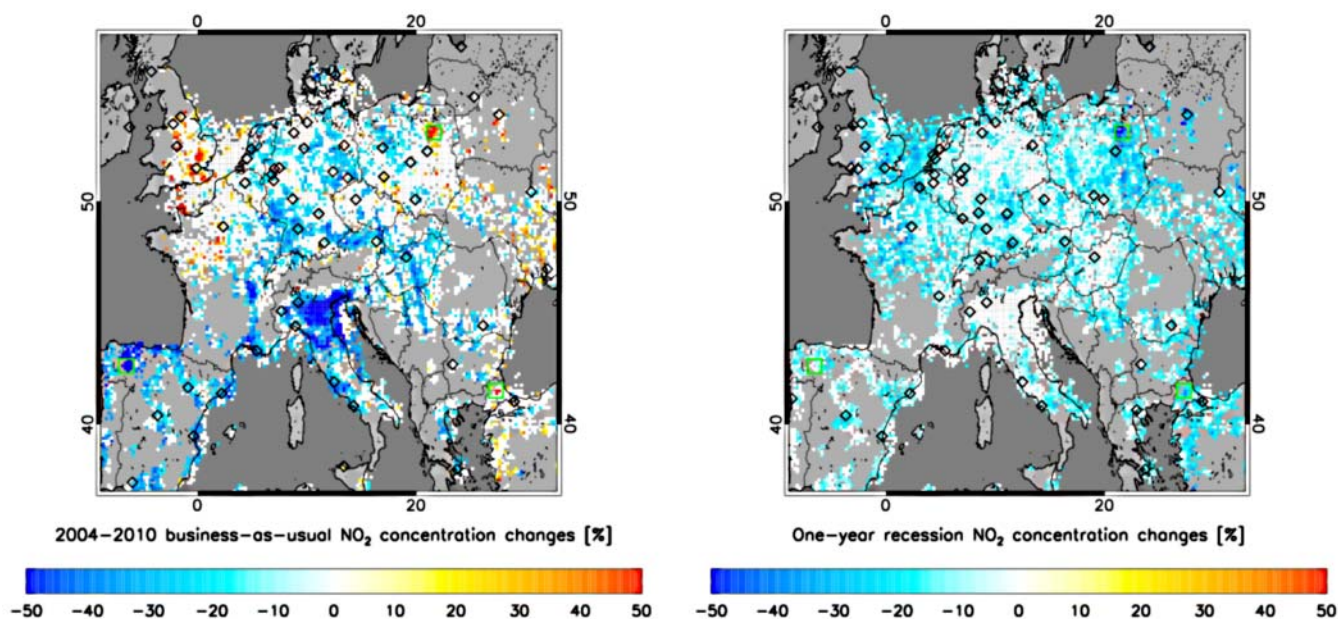


**Figure 4** | Calculated changes in NO<sub>2</sub> concentration during the OMI observation time period (October 2004–December 2010) resulting from environmental policy (‘business-as-usual’) (left) and from the 2008–2009 economic recession (right) derived from the regression model (Eqn. 1). The change in NO<sub>2</sub> is given in units of percent relative to October 2004. Calculated NO<sub>2</sub> changes that were not statistically significant (T-test,  $p=0.05$  two-tailed) were set to zero (white) in the maps. Black diamonds show the locations of cities in Europe with population greater than 500,000. Green boxes show the locations of the (1) Compostilla II power station in northwest Spain, (2) Hamitabat power station northwest of Istanbul, and (3) Ostraleka power station in northeast Poland.

$$n_{m,k}(t) = \frac{1}{m} \sum_{s=-\lfloor(m-1)/2\rfloor}^{s=\lfloor(m-1)/2\rfloor} n(t+s)$$

where  $n_{m,k=1}$  becomes the input for the second iteration of the filter, and so on. The transfer function of such a filter with  $k \geq 3$  is essentially a step function that when applied on a linear system (e.g. the signal can be modeled as the sum of signals containing different frequency components) passes frequencies below a specified value (referred to as the separating frequency). The effective separating frequency ( $p$ ) is approximately equal to  $\frac{0.5}{m \times k^{1/2}}$  [21]. Thus, by choosing an appropriate  $k$  and  $m$ , one can remove specific high frequency variations from data.

In this work, we examine the multi-year variability of NO<sub>2</sub> that is a result of applying a KZ filter of 6 iterations of a 103-day moving average ( $n_{103,6}$ ) to log-transformed (see Supplementary Information) daily data in each grid cell. This removes variations with periodicity less than approximately 1.4 years from the original signal. We choose 1.4 years as our effective separating frequency to minimize convolution of seasonal variability with long-term variability, which can occur if the effective filter width overlaps with frequencies close to one year. The effectiveness of

the separation is tested by the covariance of filtered data and its residual ( $r=n-n_{103,6}$ ). For our dataset, this is generally less than 3% of the total variance in the original signal (Figure S2). Thus, with seasonality effectively removed, variability in the filtered signal is driven by multi-year (here defined as time-scales greater than 1.4 years) changes in emissions and/or meteorology.

In Figure 3(top) we show observed monthly average concentrations and their 12-month running mean averaged over the eastern United Kingdom, Belgium, Luxembourg, and the Netherlands (see white box in Figure 2(top left)). We have also overlaid the corresponding average KZ-filtered signal. The absolute value of the KZ-filtered signal is offset because, as discussed in Supporting Information - ‘Spectral Analysis: Log Transformation’, the product of the long-term and higher variability signals reproduces the total signal. The KZ-filtered signal and 12-month running mean follow a similar pattern overall; there is an indication of a downward trend in NO<sub>2</sub> concentration in both curves, but year-to-year changes are more difficult to discern from the 12-month running mean. NO<sub>2</sub> concentrations in this part of northern Europe lack deterministic variability such as seasonality. The main driver of NO<sub>2</sub> fluctuations is high frequency synoptic variability (timescales less than 3 months), which is apparent in the monthly

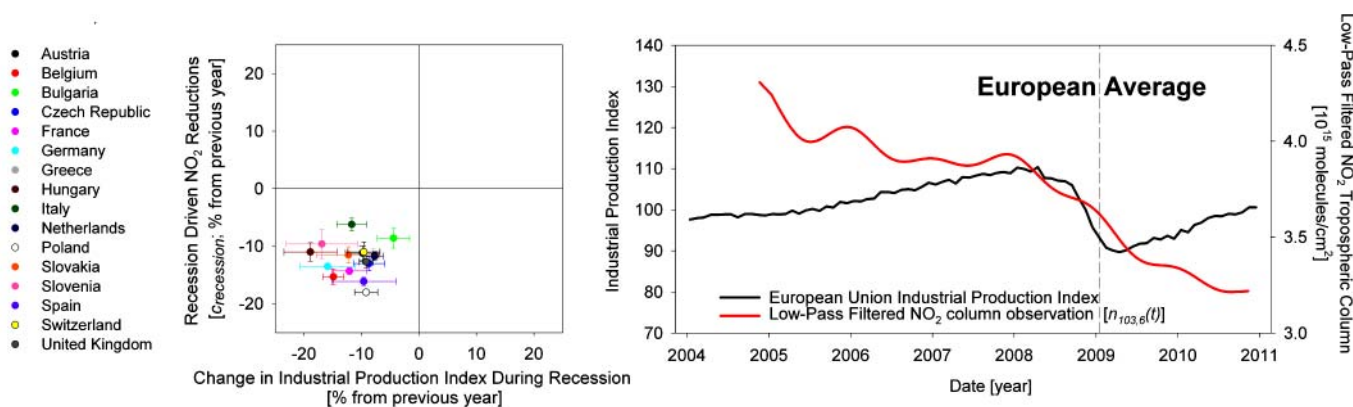


**Figure 5** | The time series of industrial production index for the 27 European Union countries, and low-pass filtered NO<sub>2</sub> tropospheric column ( $n_{103,6}$ ) averaged over the considered domain (right). The dashed line indicates the average estimated mid-date of the recession time period over Europe. The scatter plot (left) shows the recession period change in industrial production index relative to the previous year plotted against the calculated yearlong recession period change in NO<sub>2</sub> ( $c_{recession}$ ) relative to the previous year for countries in Europe.

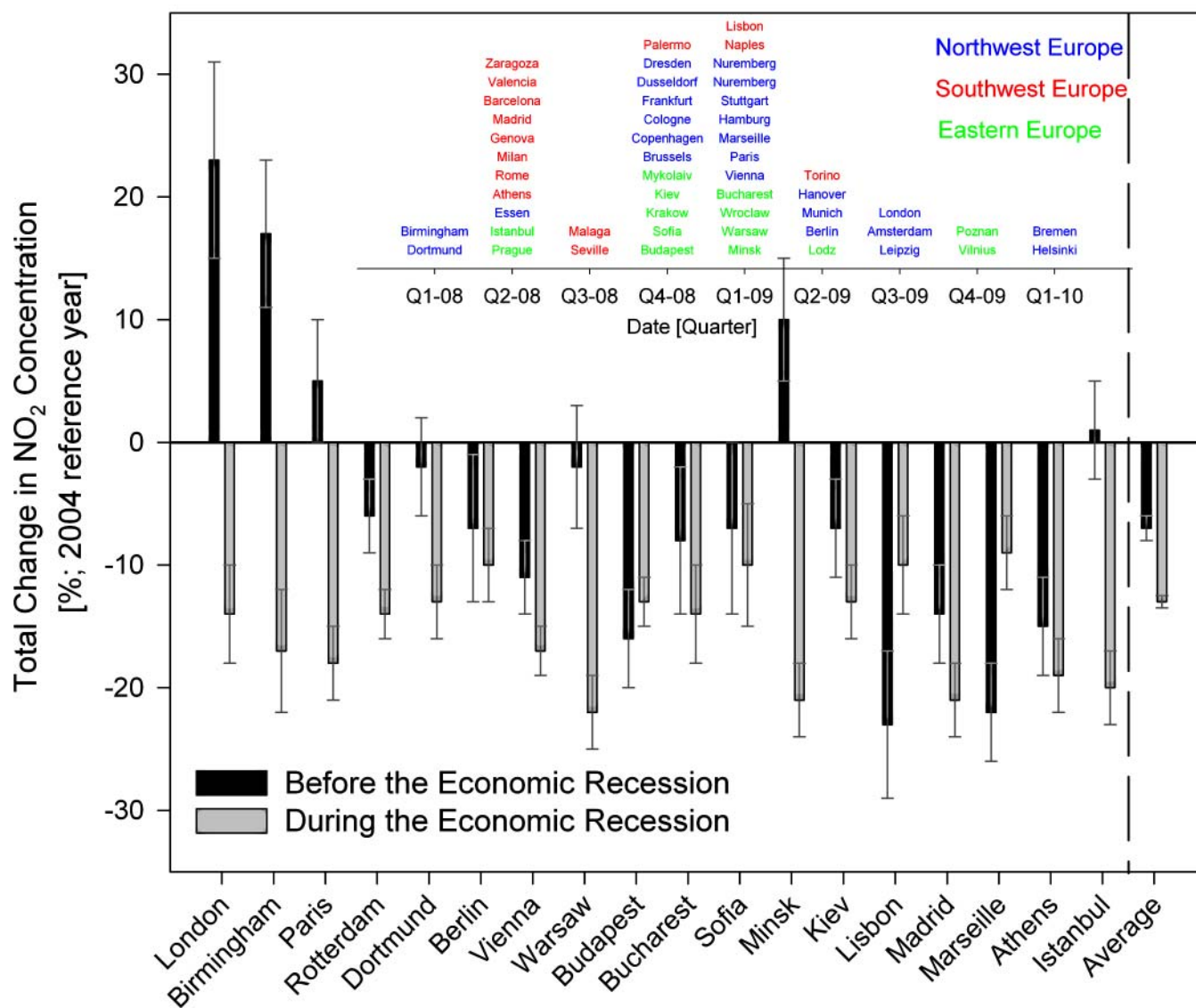


**Figure 6** | The calculated total relative change in NO<sub>2</sub> concentration before and during the economic recession for 18 large European cities with more than 500,000 inhabitants. Black bars indicate the total relative change in NO<sub>2</sub> between 2004 and the estimated start of the economic recession (the business-as-usual time period where economic growth is offset by environmental policy). Grey bars indicate the change in NO<sub>2</sub> during the yearlong economic recession (also relative to 2004). The average value is for all European cities with populations greater than 500,000 (see Figure S6). The areas considered for each city correspond to the average of the closest co-located grid cell and the surrounding 8 grid cells. The mid-date of the economic recession (inset city names) was estimated as the date with the observed highest rate of NO<sub>2</sub> column decrease (minimum NO<sub>2</sub> first derivative with respect to time) after 2008.

average data and is retained in the 12-month running mean. In contrast, for the case of Madrid (Figure 1), the seasonal cycle is the dominant mode of variability, and year-to-year changes are readily apparent. Thus, in order to discern long-term trends at high resolution over a large area like Europe, where the timescale of the mode of largest variability differs from region to region, we must use a time-series separation technique such as the KZ filter.

- Dunlea, E. J. *et al.* Evaluation of nitrogen dioxide chemiluminescence monitors in a polluted urban environment. *Atmos. Chem. Phys.* **7**, 2691–2704 (2007).
- European Committee for Standardization. Vol. EN 14211,2005 (2005).
- Steinbacher, M. *et al.* Nitrogen oxide measurements at rural sites in Switzerland: Bias of conventional measurement techniques. *J. Geophys. Res., [Atmos.]* **112**, D11307 (2007).
- van der A, R. J. *et al.* Trends, seasonal variability and dominant NO<sub>x</sub> source derived from a ten year record of NO<sub>2</sub> measured from space. *J. Geophys. Res., [Atmos.]* **113**, D04302 (2008).
- Konovalov, I. B., Beekmann, M., Burrows, J. P. & Richter, A. Satellite measurement based estimates of decadal changes in European nitrogen oxide emissions. *Atmos. Chem. Phys.* **8**, 2623–2641 (2008).
- Stavrakou, T., Müller, J.-F., Boersma, K. F., De Smedt, I. & van der A, R. J. Assessing the distribution and growth rates of NO<sub>x</sub> emission sources by inverting a 10-year record of NO<sub>2</sub> satellite columns. *Geophys. Res. Lett.* **35**, L10801 (2008).
- Mol, W. J. A., van Hooydonk, P. R. & de Leeuw, F. A. A. M. The state of the air quality in 2008 and the European exchange of monitoring information in 2009. Report No. ETC/ACC Technical paper 2010/1 (2010).
- Carlsaw, D. C., Beevers, S. D. & Bell, M. C. Risks of exceeding the hourly EU limit value for nitrogen dioxide resulting from increased road transport emissions of primary nitrogen dioxide. *Atmos. Environ.* **41**, 2073–2082 (2007).
- Keuken, M., Roemer, M. & Elshout, S. v. d. Trend analysis of urban NO<sub>2</sub> concentrations and the importance of direct NO<sub>2</sub> emissions versus ozone/NO<sub>x</sub> equilibrium. *Atmos. Environ.* **43**, 4780–4783 (2009).
- van der A, R. J. *et al.* Detection of the trend and seasonal variation in tropospheric NO<sub>2</sub> over China. *J. Geophys. Res., [Atmos.]* **111**, D12317 (2006).
- Richter, A., Burrows, J. P., Nüß, H., Granier, C. & Niemeier, U. Increase in tropospheric nitrogen dioxide over China observed from space. *Nature* **437**, 129–132 (2005).
- Beirle, S., Boersma, K. F., Platt, U., Lawrence, M. G. & Wagner, T. Megacity emissions and lifetimes of nitrogen oxides probed from space. *Science* **333**, 1737–1739 (2011).



13. Kim, S.-W. *et al.* NO<sub>2</sub> columns in the western United States observed from space and simulated by a regional chemistry model and their implications for NO<sub>x</sub> emissions. *J. Geophys. Res., [Atmos.]* **114**, D11301 (2009).
14. Lin, J.-T., McElroy, M. B. & Boersma, K. F. Constraint of anthropogenic NO<sub>x</sub> emissions in China from different sectors: a new methodology using multiple satellite retrievals. *Atmos. Chem. Phys.* **10**, 63–78 (2010).
15. Boersma, K. F., Eskes, H. J., Meijer, E. W. & Kelder, H. M. Estimates of lightning NO<sub>x</sub> production from GOME satellite observations. *Atmos. Chem. Phys.* **5**, 2311–2331 (2005).
16. Beirle, S., Platt, U., von Glasow, R., Wenig, M. & Wagner, T. Estimate of nitrogen oxide emissions from shipping by satellite remote sensing. *Geophys. Res. Lett.* **31**, L18102 (2004).
17. Konovalov, I. B., Beekmann, M., Richter, A. & Burrows, J. P. Inverse modelling of the spatial distribution of NO<sub>x</sub> emissions on a continental scale using satellite data. *Atmos. Chem. Phys.* **6**, 1747–1770 (2006).
18. Martin, R. V. *et al.* Global inventory of nitrogen oxide emissions constrained by space-based observations of NO<sub>2</sub> columns. *J. Geophys. Res., [Atmos.]* **108**, 4537 (2003).
19. Levelt, P. *et al.* The Ozone Monitoring Instrument. *IEEE Trans. Geo. Rem. Sens.* **44**, 1093–1101 (2006).
20. Boersma, K. F. *et al.* Near-real time retrieval of tropospheric NO<sub>2</sub> from OMI. *Atmos. Chem. Phys.* **7**, 2103–2118 (2007).
21. Rao, S. T. *et al.* Space and time scales in ambient ozone data. *B. Am. Meteorol. Soc.* **78**, 2153–2166 (1997).
22. De Smedt, I., Stavrou, T., Müller, J.-F., van der A, R. J. & Roozendael, M. v. Trend detection in satellite observations of formaldehyde tropospheric columns. *Geophys. Res. Lett.* **37**, L18808 (2010).
23. European Commission. *European economic statistics*. (2011).
24. Vestreng, V. *et al.* Evolution of NO<sub>x</sub> emissions in Europe with focus on road transport control measures. *Atmos. Chem. Phys.* **9**, 1503–1520 (2009).
25. Lamsal, L. N. *et al.* Application of satellite observations for timely updates to global anthropogenic NO<sub>x</sub> emission inventories. *Geophys. Res. Lett.* **38**, L05810 (2011).
26. European Environment Agency. Nitrogen oxides (NO<sub>x</sub>) emissions (APE 002) - Assessment. (2010).
27. Huszar, P. *et al.* Modeling the regional impact of ship emissions on NO<sub>x</sub> and ozone levels over the Eastern Atlantic and Western Europe using ship plume parameterization. *Atmos. Chem. Phys.* **10**, 6645–6660 (2010).
28. Dirksen, R. J. *et al.* Evaluation of stratospheric NO<sub>2</sub> retrieved from the Ozone Monitoring Instrument: Intercomparison, diurnal cycle, and trending. *J. Geophys. Res., [Atmos.]* **116**, D08305 (2011).
29. Braak, R. Row Anomaly Flagging Rules Lookup Table. TN-OMIE-KNMI-950 (KNMI, 2010).
30. Zurbenko, I. G. *The Spectral Analysis of Time Series*. (North Holland, 1986).

### Author contributions:

P.C. and K.F.B. conducted the analysis and wrote the manuscript.

### Additional information

Supplementary information accompanies this paper at <http://www.nature.com/scientificreports>

**Competing financial interests:** The authors declare no competing financial interests.

**License:** This work is licensed under a Creative Commons Attribution-NonCommercial-ShareAlike 3.0 Unported License. To view a copy of this license, visit <http://creativecommons.org/licenses/by-nc-sa/3.0/>

**How to cite this article:** Castellanos, P. & Boersma, K.F. Reductions in nitrogen oxides over Europe driven by environmental policy and economic recession. *Sci. Rep.* **2**, 265; DOI:10.1038/srep00265 (2012).